



HAL
open science

Plasticity of Dopaminergic Phenotype and Locomotion in Larval Zebrafish Induced by Brain Excitability Changes during the Embryonic Period

Sandrine Bataille, Hadrien Jalaber, Ingrid Colin, Damien Remy, Pierre Affaticati, Cynthia Froc, Jean-Pierre Levraud, Philippe Vernier, Michaël Demarque

► **To cite this version:**

Sandrine Bataille, Hadrien Jalaber, Ingrid Colin, Damien Remy, Pierre Affaticati, et al.. Plasticity of Dopaminergic Phenotype and Locomotion in Larval Zebrafish Induced by Brain Excitability Changes during the Embryonic Period. *eNeuro*, 2023, 10 (6), pp.0320-21. 10.1523/ENEURO.0320-21.2023 . hal-04178115

HAL Id: hal-04178115

<https://hal.science/hal-04178115>

Submitted on 1 Sep 2023

HAL is a multi-disciplinary open access archive for the deposit and dissemination of scientific research documents, whether they are published or not. The documents may come from teaching and research institutions in France or abroad, or from public or private research centers.

L'archive ouverte pluridisciplinaire **HAL**, est destinée au dépôt et à la diffusion de documents scientifiques de niveau recherche, publiés ou non, émanant des établissements d'enseignement et de recherche français ou étrangers, des laboratoires publics ou privés.



Distributed under a Creative Commons Attribution 4.0 International License

Neuronal Excitability

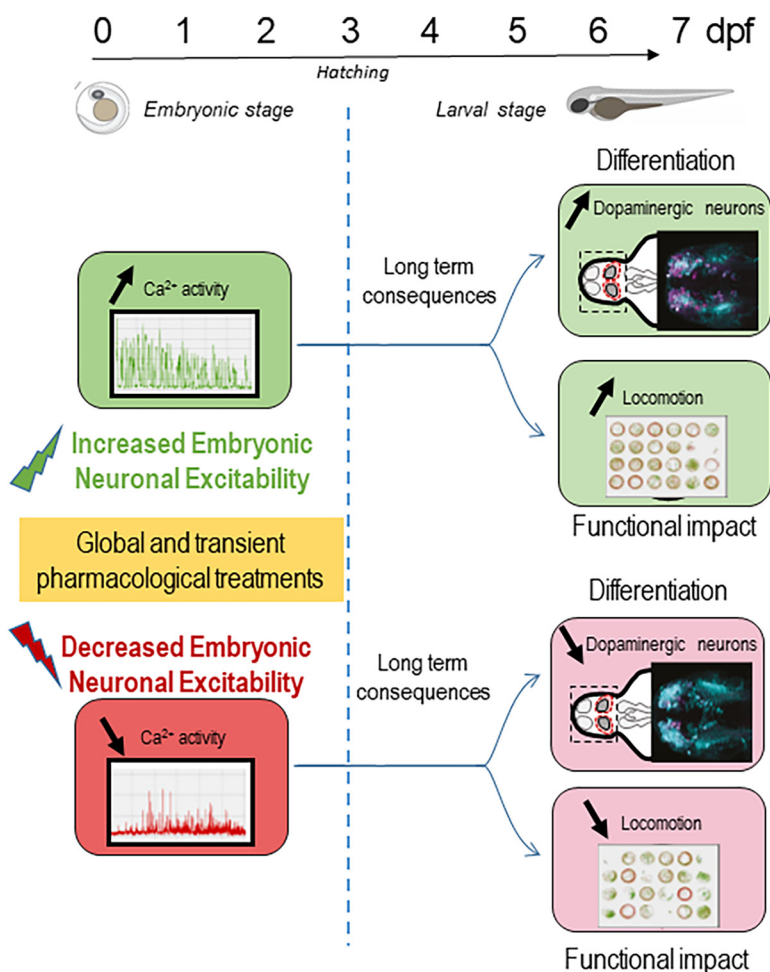
Plasticity of Dopaminergic Phenotype and Locomotion in Larval Zebrafish Induced by Brain Excitability Changes during the Embryonic Period

Sandrine Bataille,^{1,*} Hadrien Jalaber,^{1,*} Ingrid Colin,^{1,*} Damien Remy,¹ Pierre Affaticati,² Cynthia Froc,¹ Jean-Pierre Levrud,³ Philippe Vernier,¹ and  Michaël Demarque¹

<https://doi.org/10.1523/ENEURO.0320-21.2023>

¹Université Paris-Saclay, Centre National de la Recherche Scientifique, Institut des Neurosciences Paris-Saclay, Saclay 91400, France, ²Université Paris-Saclay, Centre National de la Recherche Scientifique, Institut national de recherche pour l'agriculture, l'alimentation et l'environnement, Trangénèse pour les Etudes Fonctionnelles chez les ORganismes modèles Paris-Saclay, Saclay 91400, France, and ³Université Paris-Saclay, Centre National de la Recherche Scientifique, Institut Pasteur, Université Paris-Cité, Institut des Neurosciences Paris-Saclay, Saclay 91400, France

Visual Abstract



Significance Statement

Spontaneous calcium (Ca^{2+}) transients, used here as a proxy for embryonic neural excitability (ENE), are detected in the forebrain of embryonic zebrafish. Using short-term pharmacological treatments by bath application that increase or decrease ENE we detected changes in the postmitotic differentiation of the dopaminergic phenotype, occurring within a reserve pool of vMAT2-positive cells. We also report changes in locomotion, with transient increase of ENE leading to hyperlocomotion, a phenotype associated with attention deficit hyperactivity disorder (ADHD) in this model. Our results provide a convenient framework to study the molecular mechanisms linking ENE to neurotransmitter specification.

During the embryonic period, neuronal communication starts before the establishment of the synapses with alternative forms of neuronal excitability, called here embryonic neural excitability (ENE). ENE has been shown to modulate the unfolding of development transcriptional programs, but the global consequences for developing organisms are not all understood. Here, we monitored calcium (Ca^{2+}) transients in the telencephalon of zebrafish embryos as a proxy for ENE to assess the efficacy of transient pharmacological treatments to either increase or decrease ENE. Increasing or decreasing ENE at the end of the embryonic period promoted an increase or a decrease in the numbers of dopamine (DA) neurons, respectively. This plasticity of dopaminergic specification occurs in the subpallium (SP) of zebrafish larvae at 6 d postfertilization (dpf), within a relatively stable population of vMAT2-positive cells. Nondopaminergic vMAT2-positive cells hence constitute an unanticipated biological marker for a reserve pool of DA neurons that can be recruited by ENE. Modulating ENE also affected larval locomotion several days after the end of the treatments. In particular, the increase of ENE from 2 to 3 dpf promoted hyperlocomotion of larvae at 6 dpf, reminiscent of zebrafish endophenotypes reported for attention deficit hyperactivity disorders (ADHDs). These results provide a convenient framework for identifying environmental factors that could disturb ENE as well as to study the molecular mechanisms linking ENE to neurotransmitter specification.

Key words: differentiation; dopamine; locomotion; plasticity; specification; zebrafish

Introduction

During brain development, specific molecular components of synaptic neuronal communication become functional before synapse formation, such as voltage-sensitive ion channels and neurotransmitter receptors at the plasma membrane, and the release of neurotransmitters in the extracellular space (Spitzer et al., 2002). They contribute to immature forms of cellular excitability and intercellular communications that we refer to here as embryonic neural excitability (ENE). There is for instance a paracrine communication mediated by nonsynaptic receptors activated by

endogenous neurotransmitters, in the neonatal rat hippocampus, and in the mouse spinal cord (Demarque et al., 2002; Owens and Kriegstein, 2002; Scain et al., 2010). Acute changes of calcium (Ca^{2+}) concentration with different spatiotemporal dynamics have also been described in differentiating neurons, either locally, in filopodia or growth cone or globally, at the level of the soma (Gomez and Spitzer, 1999; Gomez et al., 2001). The latter, that we refer to here as Ca^{2+} transients, are sporadic, long-lasting global increases of intracellular concentration of Ca^{2+} that occur during restricted developmental windows called “critical periods.” They have been identified in the developing brain of several vertebrate species (Owens and Kriegstein, 1998; Crépel et al., 2007; Blankenship and Feller, 2010; Demarque and Spitzer, 2010; Warp et al., 2012). Changes in the incidence and frequency of Ca^{2+} transients have been shown to modulate the specification of the neurotransmitter phenotype in various populations of neurons, as is the case for dopamine (DA), in the *Xenopus* and rat brain, with consequences on several behaviors (Dulcis and Spitzer, 2008; Dulcis et al., 2013, 2017).

DA is an evolutionarily conserved monoamine involved in the neuromodulation of numerous brain functions in vertebrates, including motivational processes, executive functions, and motor control (Klein et al., 2019). Accordingly, alterations of the differentiation and function of the neurons synthesizing DA contribute to the pathogenesis of several brain diseases with a neurodevelopmental origin, such as attention deficit hyperactivity disorder (ADHD) and schizophrenia (SZ; Lange et al., 2012; Murray et al., 2017).

Received July 28, 2021; accepted May 8, 2023; First published June 14, 2023.

The authors declare no competing financial interests.

Author contributions: P.V. and M.D. designed research; S.B., H.J., I.C., D.R., P.A., C.F., and M.D. performed research; J.-P.L. contributed unpublished reagents/analytic tools; I.C. and M.D. analyzed data; J.-P.L., P.V., and M.D. wrote the paper.

This work was supported by the French National Research Agency (ANR Project “PallEnody”) and the Fondation pour la Recherche Médicale (“team FRM”).

Acknowledgments: We thank Kei Yamamoto for key scientific inputs and TEFOR Paris-Saclay (TPS) for technical support.

*S.B., H.J., and I.C. contributed equally to this work.

Correspondance should be addressed to Michaël Demarque at michael.demarque@cnrs.fr.

<https://doi.org/10.1523/ENEURO.0320-21.2023>

Copyright © 2023 Bataille et al.

This is an open-access article distributed under the terms of the Creative Commons Attribution 4.0 International license, which permits unrestricted use, distribution and reproduction in any medium provided that the original work is properly attributed.

Further addressing the complex molecular and cellular mechanisms linking developmental excitability, dopaminergic differentiation, and behavioral outputs requires an *in vivo* approach in an accessible and genetically amenable animal model. The developing zebrafish *Danio rerio* fits these needs. The development of the embryo is external, which allows perturbing ENE at stages that would be *in utero* in mammalian models. The embryos are relatively small and transparent, simplifying high-resolution imaging of the brain in live or fixed preparations. Despite differences in brain organization, notably a pallium very different from the six-layered cortex of mammals, the main neuronal systems of vertebrates are present in zebrafish and respond to psychoactive drugs (Gawel et al., 2019). In addition, the monoaminergic system has been extensively studied in zebrafish (Schweitzer and Driever, 2009; Schweitzer et al., 2012). In vertebrates, DA modulates executive functions, such as working memory and decision-making, through the innervation of specific regions of the telencephalon. In the zebrafish brain, most DA neurons innervating the telencephalon have their cell bodies located within the telencephalon itself (SP-DA cells; Tay et al., 2011; Yamamoto et al., 2011). To the best of our knowledge, the plasticity of the neurotransmitter phenotype in these cells has not been studied so far.

To perturb ENE globally, we used pharmacological treatments by bath application from 48 to 72 h postfertilization (hpf). We then analyzed the consequences of these transient pharmacological treatments a few days later, between 6 and 7 d postfertilization (dpf). We report quantifiable changes in the specification of the dopaminergic phenotype in SP-DA neurons. We also report induced changes in locomotion within the same time frame. These results suggest a contribution of ENE to the specification of the dopaminergic phenotype and the establishment of motor control in the zebrafish. They also open important perspectives for this model to decipher the molecular events leading from environmental factors to the modifications of developmental trajectories.

Materials and Methods

Fish strains

All experiments were conducted following animal care guidelines provided by the French ethical committee and under the supervision of authorized investigators.

Zebrafish were raised according to standard procedures (Westerfield, 2000). Briefly, for breeding, male and female zebrafish were placed overnight, in different compartments of a tank with a grid at the bottom that allows the eggs to fall through. The next morning the separation was removed and after a few minutes, the eggs were collected, rinsed, and placed in a Petri dish containing embryo medium (EM). Embryos were kept at 28°C, then staged according to standard criteria. The number of animals used for each experiment is indicated in the corresponding figure legends.

Wild-type zebrafish were of AB background. The following transgenic zebrafish lines were used: *Tg(hsp70l:Gal4)^{kca4}*, *Tg*

(UAS:GCaMP6f;cryaa:mCherry)^{icm06}, *Tg(tbp:Gal4;myl7:cerulean)^{f13}*, *Tg(elavl3:Gal4)^{z734}*, and *Tg(Et.slc18a2:GFP)^{z710}*.

Pharmacological treatments

Pharmacological compounds, veratridine (10 μM), tetrodotoxin (TTX; 2 μM), ω conotoxin (0.08 μM), nifedipine (0.4 μM), and flunarizine (2 μM) were purchased from R&D Systems and prepared in water except for veratridine which required dimethyl sulfoxide (DMSO) for dissolution and flunarizine that requires ethanol (EtOH) for dissolution. Control exposures were performed using the same concentration of DMSO in EM without the drug. The specific period and duration of applications are indicated in the corresponding figure legends. All pharmacological treatments were performed by bath application followed by three washes in EM. Embryos were randomly distributed in wells (30 embryos per well) of a six-well plate containing 5 ml of solution (EM+DMSO or EM+drug). Embryos exposed to drugs or the control solution were observed for morphologic abnormalities every day until 5 dpf. Malformations (e.g., spinal curvature, cardiac edema) were considered experimental end-points, and when detected the corresponding animals were excluded from the study.

Calcium imaging

For Ca^{2+} imaging, we measured the fluorescence of the genetically encoded Ca^{2+} sensor GCaMP6f, expressed under the control of a UAS promoter (*UAS:GCaMP6f*). We used three different gal4 lines to drive UAS-dependent expression of GCaMP: a (*TBP:Gal4*) line, in which the TATA-box binding protein (TBP) promoter drives constitutive ubiquitous expression of the transgene, a *Tg(hsp70l:Gal4)* line in which the expression is triggered following a transient increase in temperature, and a (*Elavl3:Gal4*) line, in which the *Elavl3* promoter drives pan-neuronal expression of the transgene.

At 24 hpf, embryos of the (*Hsp70:GAI4;UAS:GCaMP6f*) line were exposed to a 38°C temperature for 1.5 h. Upon heat shock activation, GCaMP6f is expressed in all the cells of the animals and remains detectable for several days.

At 2–3 dpf, the embryos were paralyzed with intramuscular injections of 750 $\mu\text{g}/\text{ml}$ α -bungarotoxin (Life Technologies), then individually embedded in low melting agarose (Life Technologies), ventral side up, for imaging.

Thirty-minute time-lapse series were acquired at 1 Hz, at a single focal plane, on an Olympus BX60 microscope (Olympus Corporation) equipped with a 40 \times 0.6 N water immersion objective. A nonlaser spinning disk system (DSD2, ANDOR Technology) was used for illumination and image acquisition. Images were processed with Fiji. Movements of the preparation in the *x*-/*y*-axis were corrected using the “Stackreg” plugin (W. Rasband, B. Dougherty). Regions of interest (ROIs) were drawn manually over individual cell bodies and the average gray level from pixels in ROIs was measured over time using the MultiMeasure plugin (Optinav). Sequential values of fluorescence were then treated in MATLAB (MathWorks). Transients were defined

as an increase of fluorescence higher than 2.5 times the standard deviation of the baseline. The duration and amplitude of transients were calculated using the “peak” function. Incidence was scored as the number of cells generating transients divided by the estimated total number of cells in the imaged field and was expressed as a percentage. Frequency was calculated as the total number of transients in a given cell divided by the total acquisition time and was expressed as transients per hour.

Immunohistochemistry

Tissue preparations

Six- to 7-dpf zebrafish larvae were deeply anesthetized using 0.2% Ethyl3-aminobenzoate methanesulfonate (MS222; Merck KGaA) diluted in EM, then they were fixed in ice-cold 4% paraformaldehyde (PFA; Electron Microscopy Sciences) in 1× PBS (Fisher Scientific) containing 0.1% Tween 20 (PBST) overnight at 4°C. Samples were dehydrated and stored in MeOH at −20°C.

Immunofluorescence

Immunofluorescence was performed in 2-ml microtubes. Unless specified otherwise in the protocol, incubations were performed at room temperature (RT), and thorough PBST washes were performed between each step. The samples were first incubated in 3% hydrogen peroxide (H₂O₂) solution in ethanol (EtOH) 100% for 30 min, to deactivate endogenous peroxidases. They were then successively incubated in EtOH:Xylene 1:1 without agitation for 1 h and, at −20°C, in EtOH:acetone 1:2 without agitation for 20 min. The washes performed between these steps were performed in EtOH. After the final wash, samples were rehydrated in PBST.

To unmask the antigens, samples were incubated in PBST:Tris 150 mM pH 9 for 10 min, then in Tris 150 mM pH 9 at RT for 10 min and at 70°C for 30 min. After PBST washes, the samples were incubated in blocking buffer 1 [10% normal goat serum (NGS), 1% Triton X-100, 1% Tween 20, 1% DMSO, 1% bovine serum albumin (BSA) in PBS 1×] for 3 h.

Two protocols were used for primary antibody staining, adapted from published protocols (Inoue and Wittbrodt, 2011; Xavier et al., 2017; Bloch et al., 2019). For the TH antibody, the samples were incubated with the first primary antibody (mouse anti-TH, 1:250; Yamamoto et al., 2010) in primary staining solution (1% NGS, 1% Triton X-100, 1% DMSO, 1% BSA, 0.05% azide sodium in PBST) at 4°C for 7–10 d, under gentle agitation. After washing, the samples underwent a step of refixation in PFA 4% for 2 h at RT and were washed overnight in PBST.

The samples were then incubated in blocking buffer 2 (4% NGS, 0.3% Triton X-100, 0.5% DMSO in PBST) for 1 h at RT and incubated with a first secondary antibody (anti-mouse biotinylated, 1:200; Alunni et al., 2013) in secondary staining buffer (4% NGS, 0.1% Triton X-100 in PBST) for 2.5 d at 4°C under gentle agitation.

For the revelation, we used the Vectastain ABC kit (Vector). Briefly, the AB mix was prepared by adding 10 μl of solution A and 10 μl of solution B in 1 ml PBST/1% Triton X-100. One hour after the preparation, the samples

were incubated in the AB mix for 1 h. Samples were then incubated in Tyramide-TAMRA (1:200 in PBST) for 20 min, then 0.012% H₂O₂ was added directly to the solution and the samples were incubated for an additional 50 min.

Before a second primary antibody incubation, the samples underwent a step of fixation in PFA 4% for 2 h at RT and were washed overnight in PBST.

For the other primary antibodies (rabbit anti-caspase3, 1:500 or chicken anti-GFP, 1:500; Xavier et al., 2017), the samples were incubated in blocking buffer 1 for 3 h, then were incubated with the primary antibody in primary staining solution at 4°C for 3–4 d, under gentle agitation. After washes and refixation as above, the samples were incubated with the second secondary antibody (goat anti-chicken Alexa Fluor 488, 2 μg/ml) and DAPI 1× in PBST at 4°C for 2.5 d under gentle agitation. Samples were then washed three times in PBST and left overnight in PBST. For observation, brains were dissected and mounted between slides and coverslips in Vectashield solution (Vector).

Image acquisition

A Leica TCS SP8 laser scanning confocal microscope with a Leica HCTL Apo × 40/1.1 w objective was used to image the specimens.

The fluorescence signal was detected through laser excitation of fluorophores at 405, 488, 552, or 638 nm and detection was performed by two internal photomultipliers. Steps in the z-axis were fixed at 1 μm. Acquired images were adjusted for brightness and contrast using ImageJ/FIJI software.

Quantification of immunoreactive cells

The R software “sample” function was used to attribute a random number to each sample allowing for counting by observers blinded to the treatment group. The TH-immunoreactive and GFP-immunoreactive cells were counted manually from z-stacks of confocal images using the ImageJ cell counter plugin.

Spontaneous locomotion assays

We recorded the locomotion of individual larvae at 6–7 dpf, a period of relative stability for swimming parameters (Colwill and Creton, 2011; data not shown). larvae were placed in wells of 24-well plates with 2 ml of EM 2 h before the recordings for habituation. The plate were then placed on an infrared floor, under an infrared-sensitive camera (ZebraBox, Viewpoint) for 10-min recording sessions. Locomotor activity was recorded using ZebraLab software (Videotrack; ViewPoint Life Sciences). We first performed sessions with anesthetized larvae using several thresholds to help determine the minimum value allowing removing noise from the movement dataset. A 1.5 mm.s^{−1} low limit led to the elimination of >90% of quantification not related to active specimen movement (data not shown). This value was used as a low threshold in subsequent analysis.

One characteristic of larval swimming behavior is the presence of high-speed swimming episodes called bursts.

They are classically defined as swimming episodes with a speed higher than $20 \text{ mm}\cdot\text{s}^{-1}$ (Budick and O'Malley, 2000). We therefore used this value as a high threshold to distinguish burst from cruise episodes in our analysis.

For the experimental sessions, we assessed the distance covered by the larvae without using thresholds. We then analyzed the distance covered during cruises, i.e., during episodes with a speed between 1.5 and $20 \text{ mm}\cdot\text{s}^{-1}$ and the distance covered associated with bursts, i.e., during episodes with a speed $>20 \text{ mm}\cdot\text{s}^{-1}$. Each data point correspond to the distance covered by a larva during the entire experimental session.

Statistical analyses

Results are shown as scatterplots overlaid with box and whisker plots showing minimum (bottom whisker), maximum (top whisker), mean (cross), median (line), first quartile (bottom of the box), and third quartile (top of the box), and each value (dots). For means comparisons, we first performed the Shapiro–Wilk test for normality. If all samples passed the normality test, we then checked for equality of variance. When all samples had similar variances, we performed an ordinary ANOVA test. When differences in variances were detected, we performed Brown–Forsythe and Welch ANOVA tests (BFW ANOVA). Multiple comparisons were then performed using Dunnett's test. If one sample or more did not pass the normality test, we used the nonparametric Kruskal–Wallis test coupled with Dunn's test for multiple comparisons (KW). Tests and p values are in the figure legends; $p < 0.05$ was considered as the level for significance and is reported as follows on graphs: * $p < 0.05$, ** $p < 0.01$, *** $p < 0.001$, **** $p < 0.0001$ (ns = non significant).

Statistical tests were performed using Prism (GraphPad), except for the equality of variance test performed with the online software Brightstat (Stricker, 2008).

Results

Timing of experiments

To study the contribution of embryonic neural excitability (ENE) to zebrafish larval development, we adapted the transient pharmacological treatments previously validated in *Xenopus* (Borodinsky et al., 2004). Bath treatments were performed during the last day of embryonic development (48–72 hpf) to avoid effects on early developmental steps such as neurulation. The acute effect of the treatments were assessed by calcium imaging during the course of the treatments, while their long-term effects were studied by immunohistochemical and behavioral analysis at 6–7 dpf, several days after the washes (Fig. 1A). To increase ENE we used veratridine ($10 \mu\text{M}$), which blocks the inactivation of voltage-dependent sodium channels. To decrease ENE, we used a cocktail containing TTX ($2 \mu\text{M}$), ω -conotoxin ($0.08 \mu\text{M}$), nifedipine ($0.4 \mu\text{M}$), and flunarizine ($2 \mu\text{M}$) targeting voltage-dependent sodium channels, N, L, and T subtypes of voltage-dependent Ca^{2+} channels, respectively. We refer to this cocktail as TCNF.

Spontaneous calcium transients in the brain of zebrafish embryos

To evaluate the level of ENE in the embryonic zebrafish brain, we used Ca^{2+} transients as a proxy. We followed the dynamics of intracellular Ca^{2+} concentration using time-lapse imaging of 2- to 3-dpf zebrafish embryos expressing the genetically encoded Ca^{2+} reporter GCaMP6f (Fig. 1B,C). Because of the noncell autonomous mechanism involved in the plasticity of the neurotransmitter phenotype described in *Xenopus* (Gomez-Gamboa et al., 2014), we used ubiquitous reporters to detect changes in fluorescence in all telencephalic cells. To induce UAS-dependent GCaMP6f expression, we first used the (*Hsp70:Gal4* x *UAS:GCaMP6f;cry:mCherry*) line, in which the transgene is expressed on heat shock activation (see Materials and Methods; Fig. 1D–G). To ensure that the observed phenotypes were not altered by the initial heat shock, we confirmed these results using a *TBP:Gal4* driver, in which the TATA-box binding protein (TBP) promoter (Burket et al., 2008) drives constitutive transgene expression (Fig. 1H–K). To confirm that neurons were contributing to a majority of the pattern observed we repeated the experiments using a pan-neuronal reporter (*elavl3:Gal4*; Fig. 1L–O).

To monitor changes in fluorescence over time, we imaged of the anterior-most part of the brain of 2- to 3-dpf zebrafish embryos for 30-min sessions. We analyzed the evolution of the fluorescence from selected regions of interest (ROIs) corresponding to individual cell bodies. We used four parameters to analyze the results, the average frequency of transients per ROI, the incidence of active ROIs in the field of view (number of ROIs displaying at least one transient during the recordings over the estimated total number of ROIs), and the duration and amplitude of individual transients (Materials and Methods). In control conditions, we detected the presence of sporadic spontaneous transients in the telencephalon of the three transgenic backgrounds we used (Fig. 1D–O, blue symbols). The analyzed parameters were in the range of what has been reported in the *Xenopus* brain (Dulcis and Spitzer, 2008; Demarque and Spitzer, 2010) and longer than what has been reported for the embryonic zebrafish spinal cord (Warp et al., 2012; Plazas et al., 2013).

Global pharmacological modifications of the dynamic of calcium transients

To assess the ability of our pharmacological treatments to modify ENE, we measured their impact on Ca^{2+} signaling. We performed time-lapse recordings 2–10 h after the addition of the treatments to the embryo medium. Here again, the results obtained were similar in the three genetic backgrounds. Following veratridine treatment, the four parameters analyzed were increased (Fig. 1D–O, green symbols). In contrast, following TCNF treatments, three of the analyzed parameters were decreased, frequency, incidence, and amplitude while the duration was increased (Fig. 1D–O, red symbols).

These results demonstrate that bath-mediated pharmacological treatments were able to change the incidence, frequency, and amplitude of spontaneous Ca^{2+} transients

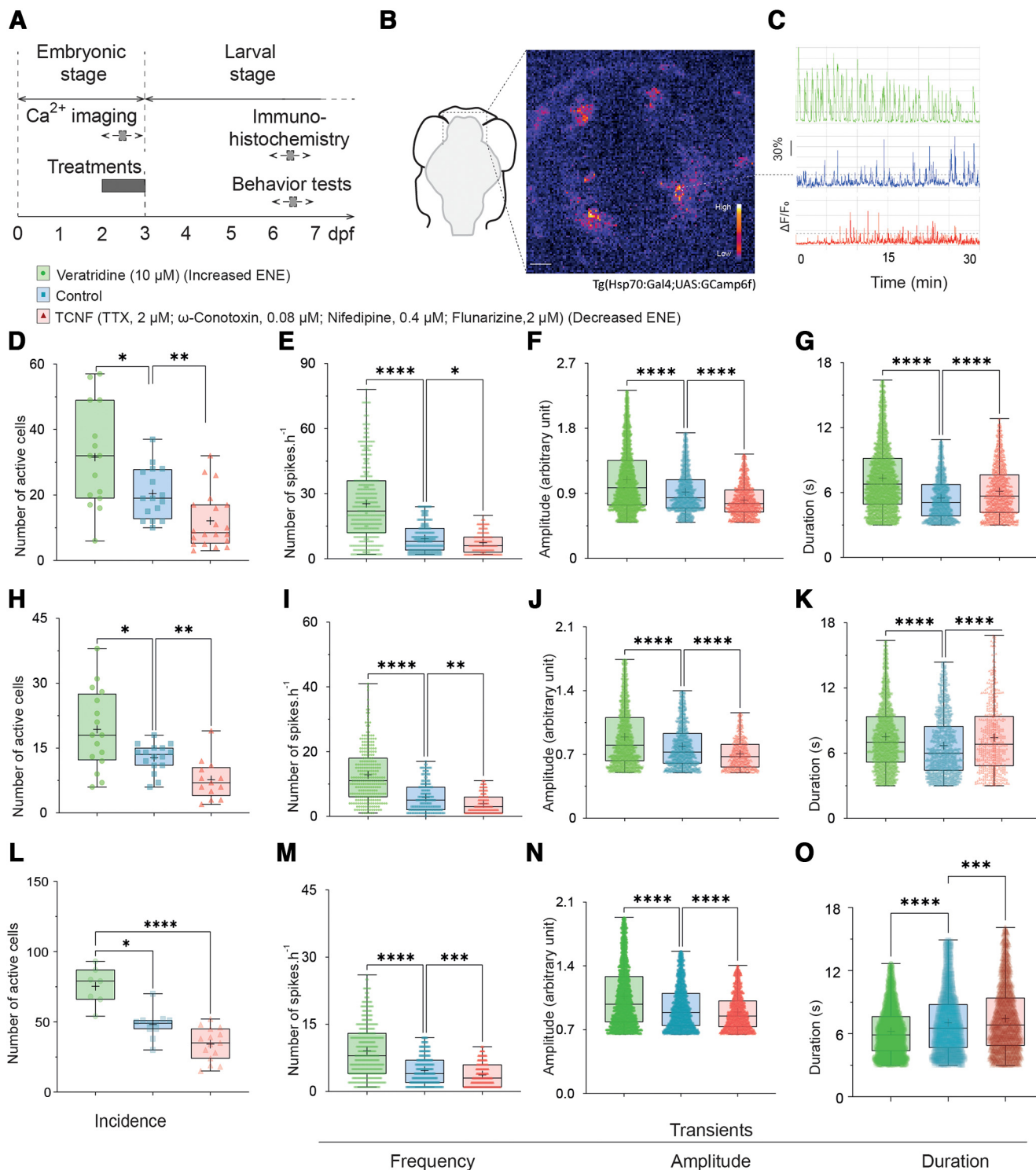


Figure 1. Timing of the experiments, characterization of forebrain calcium transients and their modification by bath application of pharmacological treatments. **A**, Timeline of the experiments. Pharmacological treatments and calcium imaging experiments were performed from 2 to 3 dpf (embryonic period) and the immunohistochemistry and behavior experiments were performed several days later, at 6–7 dpf (larval period). **B**, Left panel, Schematic ventral view of a zebrafish brain, showing the approximate region for calcium recordings. Right panel, Confocal image from a time-lapse recording of the brain of 48 hpf of *Et(hsp:gal4;UAS:GCamp6f)* embryos in control conditions. Fluorescence is displayed on a pseudocolor scale, the lookup table coding for the intensity scale is shown in the bottom-right corner of the image. Scale bar = 100 μm. White dash-circle defines an example region of interest corresponding to the cell body of a cell which changes in fluorescence are displayed in **C**. **C**, Representative changes in fluorescence intensity plotted as a function of time in different experimental conditions: control conditions in blue, following veratridine treatment (10 μM) in green, and following TCNF treatment (TTX, 2.5 μM; ω-conotoxin, 0.1 μM; nifedipine, 0.5 μM and flunarizine, 2.5 μM) in red.

continued

Ca²⁺ transients were scored as changes in fluorescence more than two times higher than the SD of the baseline (dashed lines), and >3 s in duration, calculated as the width at half-maximum. **D–O**, Boxplots showing different parameters of calcium spikes in control conditions (blue), following 10 μM veratridine treatment (green) and following TCNF treatment (red). **D–G**, Results obtained in the *Hsp:gal4* line from five independent experiments. **H–K**, Results obtained in the *TBP:gal4* line, from six independent experiments. **L–O**, Results obtained in the *HuC:gal4* line, from three independent experiments. **D**, Average incidence of the recorded Ca²⁺ transients, BFW ANOVA, 15 < *n* < 21 fields of view. **E**, Average frequency, KW test, 291 < *n* < 535 values. **F**, Average normalized amplitude of the recorded Ca²⁺ transients, KW test, 1258 < *n* < 4809 transients. **G**, Average duration of the Ca²⁺ transients, KW test, 1258 < *n* < 4809 transients. **H**, Average incidence of the recorded Ca²⁺ transients, BFW ANOVA, 13 < *n* < 17 fields of view. **I**, Average frequency, KW test, 148 < *n* < 281 values. **J**, Average normalized amplitude of the recorded Ca²⁺ transients, KW test, 607 < *n* < 2980 transients. **K**, Average duration of the Ca²⁺ transients, KW test, 607 < *n* < 2980 transients. **L**, Average incidence of the recorded Ca²⁺ transients, BFW ANOVA, 7 < *n* < 15 fields of view. **M**, Average frequency, KW test, 507 < *n* < 527 values. **N**, Average normalized amplitude of the recorded Ca²⁺ transients, KW test, 2442 < *n* < 5149 transients. **O**, Average duration of the Ca²⁺ transients, KW test, 2442 < *n* < 5149 transients. **p* < 0.05, ***p* < 0.01, ****p* < 0.001, *****p* < 0.001, ns = non significant.

in the embryonic zebrafish forebrain. When analyzing the late consequences of these transient treatments, we refer to the veratridine treatment as “increased ENE,” and to TCNF treatment as “decreased ENE.”

Dopaminergic cells in the telencephalon at larval stages

Next, we studied the effect of the transient perturbations of ENE on the maturation of the telencephalic dopaminergic (Tel-DA) neurons distributed as two neighboring subpopulations, in the subpallium (SP), and in the olfactory bulb (OB).

To identify dopaminergic neurons in the telencephalon of 6- to 7-dpf larvae we used anatomic landmarks such as the position of brain ventricles and large fiber bundles combined to two markers of the catecholaminergic phenotype: the enzyme limiting the synthesis of catecholamines (i.e., dopamine, adrenaline, and noradrenaline), tyrosine hydroxylase (TH), and the transporter accumulating monoamines inside exocytotic vesicles, vesicular monoamine transporter (vMAT). Indeed, in zebrafish, like in mammals, adrenaline and noradrenaline-containing neuronal soma, labeled by the same markers, are not detected anterior to the midbrain-hindbrain boundary, rather, they are restricted to neuronal subpopulations located in the locus coeruleus, the medulla oblongata and the area postrema (Ma, 1994a,b 1997, 2003). Thus, all the catecholaminergic neurons located anterior to the midbrain-hindbrain boundary are likely dopaminergic neurons.

In zebrafish, TH is encoded by two paralogous genes (*th1*; previously known as *th1* and *th2*). *th2* is mostly expressed in the caudal hypothalamus and is very rare in the nuclei studied here (Panula et al., 2010). We, therefore, used an anti-TH antibody that identifies Th-expressing cells (referred to as TH1⁺ cells in the remaining manuscript) but does not recognize Th2 (Yamamoto et al., 2011). vMAT is encoded by two different genes (*slc18a1* and *slc18a2*, also known as *vmat1* and *vmat2*), but only the latter is detected in the zebrafish brain (Puttonen et al., 2017), so we used an anti-GFP antibody to amplify the endogenous GFP signal from cells in the *Tg(Et.vMAT2:eGFP)* transgenic line (referred to as vMAT2⁺ cells in the remaining of the manuscript).

In the SP, the cell bodies of vMAT2⁺ cells (hereafter noted SP-vMAT2⁺ cells) were distributed bilaterally along the midline, and relatively close to it (Fig. 2A, cyan labeling). The majority of fibers we could detect projected first ventrally and then laterally, joining the wide dopaminergic lateral longitudinal tracts.

In the OB, the cell bodies of vMAT2⁺ cells (noted OB-vMAT2⁺ cells) were distributed at the anterior end of the forebrain and were projecting anteriorly before rapidly branching in multiple directions.

In both regions, the overall disposition of the TH1⁺ cell bodies and projections were similar as for vMAT2⁺ cells. All TH1⁺ cells were also vMAT2⁺, while some vMAT2⁺ cells were TH1⁻ (Fig. 2A, magenta labeling). In the SP, vMAT2⁺/TH1⁻ cell bodies were mostly located at the anterior end of the cluster of vMAT2⁺/TH1⁺ cells. Such vMAT2⁺/TH1⁻ cells are also detected in the SP of adult zebrafish (Yamamoto et al., 2011). The proportion of TH1⁺ cells over vMAT2⁺ cells was 38.9 ± 2.9% in the SP and 74.2 ± 3.1% in the OB (Fig. 2C,E).

Effects of modification of ENE on the expression of dopaminergic markers in the telencephalon and the OB

To assess the effects of ENE on the expression of the dopaminergic markers in the telencephalon at larval stages, we counted the number of vMAT2⁺ and TH1⁺ cells in larvae fixed at 6–7 dpf, following the transient pharmacological treatments intended to increase or to decrease ENE.

In the SP, enhancing ENE from 48 to 72 hpf increased the number of TH1⁺ cells detected while lowering ENE decreased the number of TH1⁺ cells (Fig. 2A,B). In both experimental situations, the number of vMAT2⁺ cells did not change significantly despite a similar trend. Again, all SP-TH1⁺ cells also exhibited vMAT2 labeling. The proportion of TH1⁺ cells over vMAT2⁺ cells increased to 49.7 ± 6.8% following increase of ENE and decreased to 31.5 ± 3.9% following decrease of ENE, in both cases a significant difference from controls (Fig. 2A,C). Hence, according to our identification criteria (anatomic position combined with the expression of both TH1 and vMAT2), increasing embryonic electrical

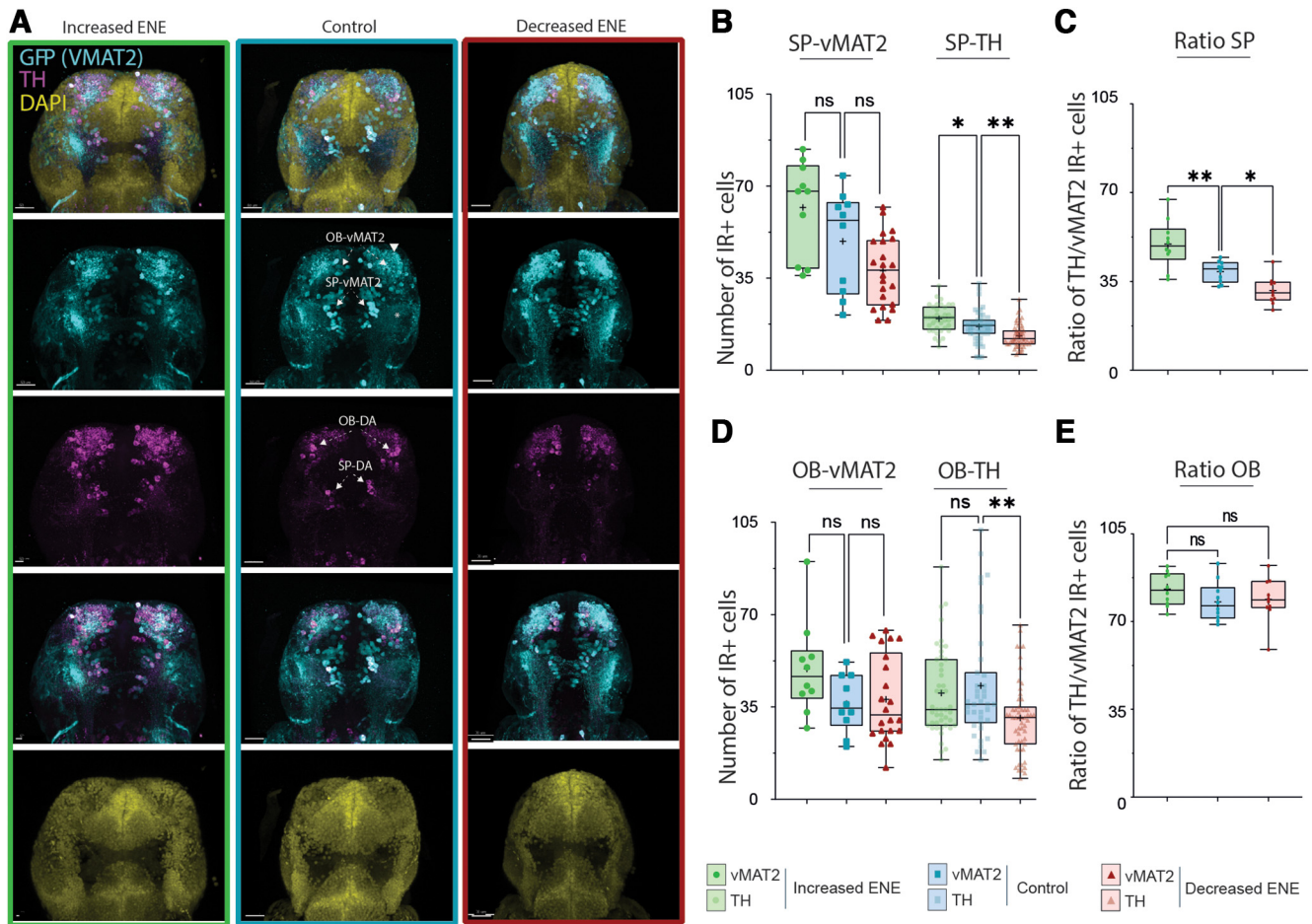


Figure 2. Effects of ENE on the expression of dopaminergic markers in the zebrafish larval subpallium and olfactory bulb. **A**, Maximum projection of confocal z series of the brain of 6- to 7-dpf *Tg(Et.vMAT2:eGFP)* larvae, following ENE increase (left column, boxed in green), in control conditions (middle column, boxed in blue), and following ENE decrease (right column, boxed in red). Immunostaining to TH (magenta) and GFP (cyan) and DAPI (yellow) are shown as composite image (top) as well as for each color channels. Scale bars = 50 μ m. **B-E**, Boxplots showing the number of cells IR⁺ for dopaminergic markers in the SP (**B**) and the OB (**D**) from six independent experiments, in control conditions (blue), following ENE increase (green) and following ENE decrease (red). **B**, Left, Number of SP-vMAT2⁺ cells, KW test, 6 < *n* < 16. Right, Number of SP-TH⁺ cells, KW test, 34 < *n* < 49. **C**, Proportion of vMAT2⁺ cells being also TH⁺ in the SP, ANOVA test, *n* = 24. **D**, Left, Number of OB-vMAT2⁺ cells, KW test, 6 < *n* < 16. Right, OB-TH⁺ cells, KW test, 34 < *n* < 49. **E**, Proportion of vMAT2⁺ cells being also TH⁺ in the SP, ANOVA test, *n* = 24. **p* < 0.05, ***p* < 0.01, ns = non significant.

activity results in more SP-DA cells in larvae, while decreasing it reduces this population.

In the OB, increasing ENE from 48 to 72 hpf did not change the number of TH⁺ cells detected while decreasing ENE significantly reduced the number of TH⁺ cells (Fig. 2A,D). As in the SP, all TH⁺ cells exhibited vMAT2 labeling, independently of the treatments. Meanwhile, the number of vMAT2⁺ cells did not change significantly in this region (Fig. 2A,D). The proportion of TH⁺ cells over vMAT2⁺ cells did not change as well (Fig. 2E). Overall, our results indicate that the number of dopaminergic (TH⁺) neurons in the larval telencephalon is positively affected by electrical activity during the embryonic stage. Modulating ENE has a much weaker impact on the size of the monoaminergic (vMAT2⁺) subpopulations. This suggests that ENE influences the specification of monoaminergic precursors during an embryonic critical window, driving them toward the dopaminergic fate.

Modifications of ENE have no effect on apoptosis in the forebrain

To check whether these changes in the number of dopaminergic neurons were associated with programmed cell death, we counted the number of cells immunoreactive for activated caspase-3, an apoptosis marker, in the vicinity of vMAT2 expression in the SP and OB, at 6–7 dpf. The number of caspase-3⁺ cells was stable following the increase or the decrease of ENE (Fig. 3). This result strengthens the hypothesis that the changes observed in the number of TH⁺ cells are indeed linked to changes in neurotransmitter specification rather than changes in cell survival.

Effects of pharmacological treatments on the locomotion of 6- to 7-dpf larvae

To analyze the consequence of the modifications of ENE on behavior, we focused our analysis on spontaneous locomotion.

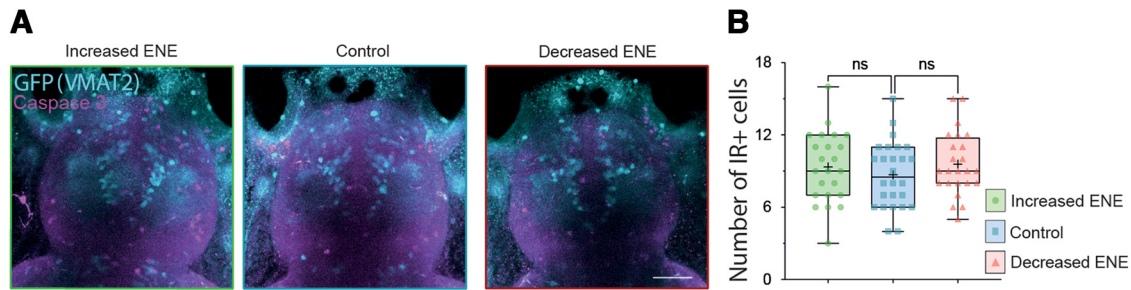


Figure 3. Absence of changes in programmed cell death following modifications of ENE. **A**, Maximum projection of confocal z series of the brain of 6- to 7-dpf *Tg(Et.vMAT2:eGFP)* larvae, following ENE increase (left image, boxed in green), in control conditions (middle image, boxed in blue), and following ENE decrease (right image, boxed in red). Immunostaining to caspase-3 (magenta) and GFP (cyan) are shown as merged channels. Scale bars = 50 μ m. **B**, Boxplots showing the number of the caspase-3⁺ IR cells counted in the telencephalon following ENE increase (green), in control conditions (blue) and following ENE decrease (red). KW test, 23 < *n* < 26 telencephalon from four independent experiments. ns = non significant.

During locomotion, zebrafish larvae display successive turn and swim bouts called episodes, interleaved with resting periods (Budick and O'Malley, 2000).

We compared locomotion parameters recorded at 6–7 dpf, >3 d after the end of ENE modifications (Fig. 1A). We recorded spontaneous locomotion of individual larvae over three consecutive 10-min sessions in each condition: control, increased ENE, and decreased ENE. A representative example of traces obtained for 24-well plates in each condition is shown in Figure 4A.

Increasing ENE increased the total distance covered by each larva (Fig. 4B, green symbols). Decreasing ENE led to a decrease of the total distance covered by each larva (Fig. 4B, red symbols).

Following this observation that modifications of ENE induced changes in spontaneous larval locomotion, we analyzed further these effects by discriminating two types of episodes based on their speed: slow and fast swimming episodes, dubbed cruises and bursts, respectively (see Materials and Methods; Budick and O'Malley, 2000; Kalueff et al., 2013). Increasing ENE increased the distance covered during both cruises and bursts (Fig. 4C,D, green symbols). Reciprocally, decreasing ENE, decreased the distance covered during both cruises and bursts (Fig. 4C,D, red symbols).

Of note, the distance covered during events with a speed below our low threshold did not change over the three experimental conditions (data not shown). Overall, increasing ENE increased locomotion while decreasing ENE decreased locomotion. Although the distinction between bursts and cruises may be viewed as arbitrary, the overall positive correlation between ENE and global larval activity (e.g., total distance swam) is robust.

Washout kinetics of pharmacological treatments assessed using locomotion parameters at 6–7 dpf and calcium signaling at 2- to 3-dpf embryos

To exclude a direct contribution of the treatments applied in the embryonic period on the parameters measured in the larval period, we assessed the reversibility of the treatments by following the time course of the effects of acute pharmacological treatments in two sets of experiments.

First, on 5-dpf larvae, we performed 10-min recording sessions and analyzed the overall distance covered before

the application of the treatments, then +2 h after the application of the treatments, and lastly 24 h after washing out the drugs. Acute treatments of swimming larvae had the expected effects: veratridine application induced an increase in the distance covered, while TCNF application led to a decrease in the distance covered (Fig. 5A, left boxplots). By the next day, all the effects of the treatments on burst episodes had faded away demonstrating the washout properties of the pharmacological agents used (Fig. 5A, right boxplots).

Second, we recorded the washout kinetics of pharmacological treatments on Ca²⁺ signals recorded in 2- to 3-dpf embryos. We applied the drugs at 48 hpf, as before. We recorded 20-min sessions between 2 and 4 h after the beginning of the applications, then washed the treatments, waited for 6–10 h, and perform new 20-min sessions (Fig. 5E,F). As described in Figure 1, after 2 h of treatment, the incidence and frequency of Ca²⁺ transients were increased by veratridine and reduced by TCNF (Fig. 5E,F, left boxplots). For both treatments, the values measured after the washing time (or washout) were back to control values (Fig. 5E,F, right boxplots).

These results indicate that washout of veratridine or TCNF results in rapid loss of direct effect of the drugs, in a few hours at most. Thus, the timing of our analysis of larval locomotion, 3 d after ENE manipulation, is far beyond the time required for the disappearance of the acute effect of the drugs. Hence, our results support the existence of a long-term effect related to changes in neural excitability during the embryonic period in the zebrafish.

Discussion

Summary

Immature forms of neural excitability, ENE, include spontaneous Ca²⁺ transients, activation of nonsynaptic receptors to neurotransmitters and early synaptic activities (Ribera and Spitzer, 1998). Our results show that the developing zebrafish is a suitable model for manipulating ENE through the use of pharmacological treatments and for studying the consequences of these manipulations on the plasticity of neuromodulator systems and their behavior. Indeed, we report that ENE exerts a positive regulatory

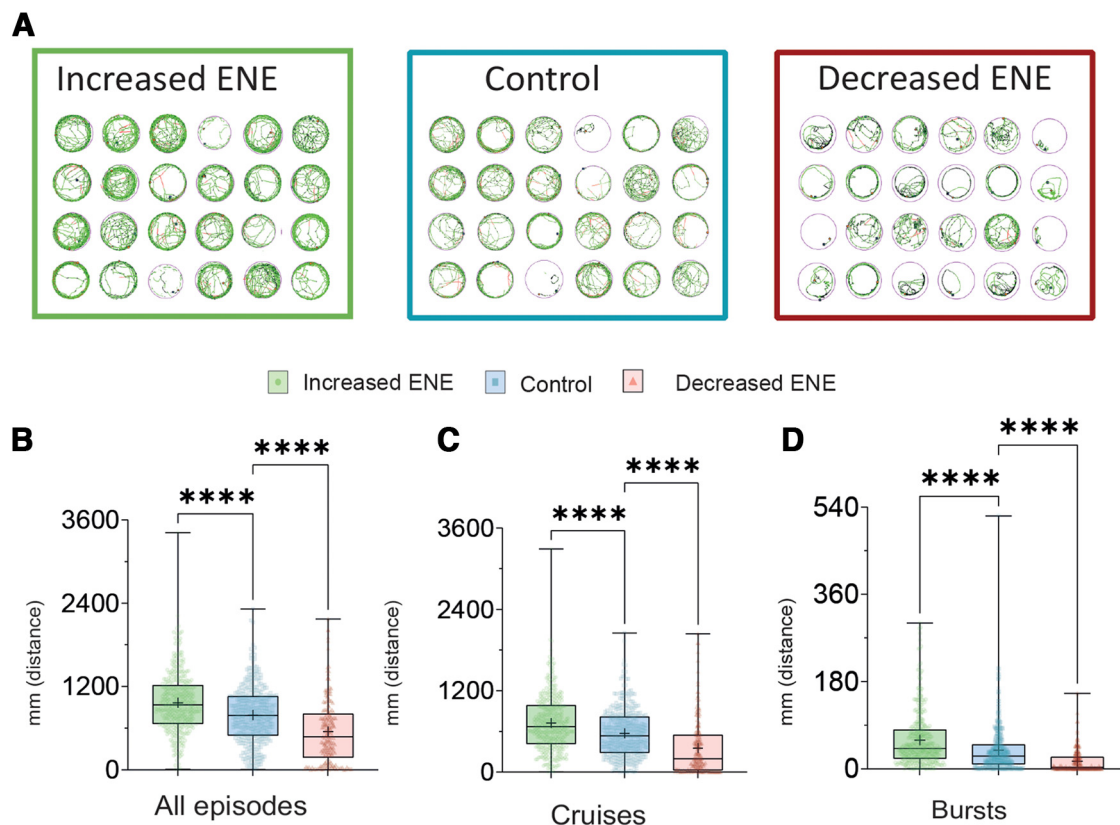


Figure 4. Effects of a 24-h bath applied treatments during embryonic development on spontaneous swimming of zebrafish larvae. **A**, Representative path reconstructions for 24 individual larvae during a 10-min trial for three experimental conditions. We performed the experiments at 6–7 dpf when the properties of swimming episodes are relatively stable in control conditions. The portion of the path corresponding to cruises episodes are shown in green, and to bursts are shown in red. **B–D**, Boxplots showing the mean distance per larva following ENE increase (green), in control conditions (blue), and following ENE decrease (red). Distance is expressed as the cumulated length of the path covered. **B**, Distance covered when no threshold is applied for the analysis. **C**, Distance covered during cruises. **D**, Distance covered during bursts. For all boxplots the p of normality test for at least one condition was <0.05 ; therefore, KW test was used, $192 < n < 384$. $****p < 0.001$.

effect on the specification of the dopaminergic phenotype by increasing the number of dopaminergic neurons in the subpallium as well as high-speed swimming episodes.

Bath application of pharmacological treatments and ENE

For the present study, zebrafish embryos were exposed to pharmacological compounds by bath application. The zebrafish is highly suitable for such questions because of its external development in an egg. In addition, our wash-out experiments agree with data in the literature indicating that the blood-brain barrier starts to form around 72 hpf but is not fully mature until 10 dpf (Fleming et al., 2013), allowing the diffusion of drugs to neural tissues during treatments and their subsequent removal on washing at embryonic stages. This methodological approach induces both global and transient effects. It helps assess the net effects of the treatments on different subpopulations of cells, in different regions of the animal. Further studies using more localized modifications of ENE could help decipher the contribution of specific brain regions.

We focused on Ca^{2+} transients, one of the main forms of immature excitability, to assess the effectiveness of the

treatments. However, other intercellular communication processes are also likely perturbed by the treatments, such as the paracrine activation of GABA and glutamate receptors by endogenous transmitters, and initial synaptic activities. Further studies are required to decipher the specific contribution of each of these mechanisms to the cellular and behavioral effects we reported here.

Calcium transients in the zebrafish subpallium

One reason to focus on Ca^{2+} transients is that they are conveniently measured by Ca^{2+} imaging. In addition, they have been previously involved in neurotransmitter phenotype specification in other models of neuronal plasticity. For example, in the developing *Xenopus* spinal cord, these Ca^{2+} transients induce the release of brain-derived neurotrophic factor (BDNF), which result in noncell-autonomous phenotype switching (Gomez-Gamboa et al., 2014). We chose to drive the expression of GCaMP ubiquitously at first to ensure we would not miss relevant cell populations at the selected period of recordings. Further studies using a pan-neuronal promoter revealed very similar patterns, leading us to conclude that activity recorded in neurons are likely accounting for the majority of the

In ecotoxicology, following exposure to modulators of activity, both direct and indirect mechanisms are likely activated and further analysis is required to disentangle their respective contributions to the phenotype plasticity reported here.

A critical period for the effect of ENE perturbations

We observed an effect of the pharmacological treatments performed during the embryonic period on spontaneous locomotion several days after the end of the treatments. In contrast, no effects were observed 24 h after treatments performed at 5 dpf in the zebrafish larvae. These long-lasting effects of treatments specifically during the embryonic period are in line with the existence of a “critical period” during development, which is more sensitive to homeostatic perturbations and promotes significant phenotypic plasticity in immature neurons. Since dopaminergic systems have multiple functional roles and are particularly prone to plasticity events (Collo et al., 2014; Macedo-Lima and Remage-Healey, 2021), this suggests that these systems might be a key factor for the adaptability of animals to environmental changes. Whether it is a cause, a consequence, or a simple correlation of their conservation throughout animal evolution is still an open question.

Identification of a biomarker for DA reserve Pool neurons

SP-DA neurons are not present in *Xenopus* and to the best of our knowledge, the plasticity of their dopaminergic phenotype has not been studied so far. In the SP, the effect of ENE perturbations on the DA phenotype analyzed by the number of TH⁺ cells was in agreement with the homeostatic rule described in *Xenopus* (Spitzer, 2012). Indeed, the DA phenotype was enhanced by increased excitability, and decreased by decreased excitability, as expected from an overall inhibitory neurotransmitter. In the OB, we observed a similar decrease of the DA phenotype following decreased excitability but no increase following increased activity. This is in contradiction to what has been reported in *Xenopus* (Velázquez-Ulloa et al., 2011). This unexpected result could be because of the number of TH⁺ cells already set at a maximum in basal conditions in the zebrafish OB as suggested by the high ratio of vMAT2⁺/TH⁺ observed in this region compare to SP in control conditions.

The relative stability of the number of vMAT2⁺ cells, together with no change in caspase 3-labeled cells on treatments, suggest that modulation of excitability did not affect cell death or proliferation, but rather influenced the commitment of precursors toward a dopaminergic fate. This plasticity of the DA phenotype is likely to occur within the pool of vMAT2⁺ cells since the number of vMAT2⁺/TH⁺ was increased with increased excitability. Therefore, the vMAT2⁺/TH⁻ cells could be a reserve pool of cells primed to become dopamine neurons when plasticity-triggering events occur. The expression of the vesicular transporter in a reserve pool of cells might have a functional advantage in terms of response to plasticity-triggering

events, limiting the number of factors to be changed for reaching a fully functional dopamine phenotype.

Behavioral consequences of ENE

Perturbations of ENE had also behavioral consequences in zebrafish larvae, modifying spontaneous locomotion. The more ENE, the higher the distance covered fitting with a contribution of dopamine. This distance was modulated for both slow and fast swimming modes (cruises and bursts), although these two behaviors are believed to involve distinct networks, suggesting that ENE should modulate a common regulatory circuit. Determining whether direct activation of dopaminergic neurons in the subpallium could stimulate cruises or bursts using optogenetic tools is an open perspective for the future. It would be interesting to test whether other behaviors such as prepulse inhibition are also affected following alterations of ENE.

Potential mechanisms linking changes in ENE and changes in locomotion

Links between movement control and the neuromodulator effect of dopamine are widely described. In zebrafish, it has been involved in the initiation of movement (Thirumalai and Cline, 2008), via direct projection from dopaminergic cells in the diencephalon (Lambert et al., 2012). Dopaminergic cells in the hypothalamus also modulate locomotion (McPherson et al., 2016). The global perturbations we used likely induced plasticity mechanisms beyond the dopaminergic cells we analyzed in this study. Changes within the spinal networks itself, and nondopaminergic modulatory networks probably occurred as well, preventing us to conclude about a causal link between the number of telencephalic DA neurons and the level of spontaneous locomotion, the two phenotypes we report here.

Perspectives: transcriptomics and model to test the impact of environmental factors on ENE

The developing zebrafish provide an attracting model in which to perform transcriptomic analysis to identify genes differentially expressed in vMAT2 cells following modifications of ENE. The results would help decipher the cellular and molecular mechanisms underlying the modulatory role of ENE during brain differentiation.

The data presented here point to an implication of ENE in the regulation of dopaminergic differentiation in the developing brain, suggesting that ENE could act as an intermediate between environmental factors and the molecular changes leading to the alteration of dopamine-related behaviors. The zebrafish model is also adapted to test how environmental factors such as malnutrition, stress, and drug exposure could modulate ENE and potentially influence the maturation of the dopaminergic systems.

References

- Alunni A, Krecsмарik M, Bosco A, Galant S, Pan L, Moens CB, Bally-Cuif L (2013) Notch3 signaling gates cell cycle entry and limits neural stem cell amplification in the adult pallium. *Development* 140:3335–3347.

- Blankenship AG, Feller MB (2010) Mechanisms underlying spontaneous patterned activity in developing neural circuits. *Nat Rev Neurosci* 11:18–29.
- Bloch S, Froc C, Pontiggia A, Yamamoto K (2019) Existence of working memory in teleosts: establishment of the delayed matching-to-sample task in adult zebrafish. *Behav Brain Res* 370:111924.
- Borodinsky LN, Root CM, Cronin JA, Sann SB, Gu X, Spitzer NC (2004) Activity-dependent homeostatic specification of transmitter expression in embryonic neurons. *Nature* 429:523–530.
- Budick SA, O'Malley DM (2000) Locomotor repertoire of the larval zebrafish: swimming, turning and prey capture. *J Exp Biol* 203:2565–2579.
- Burket CT, Montgomery JE, Thummel R, Kassen SC, LaFave MC, Langenau DM, Zon LI, Hyde DR (2008) Generation and characterization of transgenic zebrafish lines using different ubiquitous promoters. *Transgenic Res* 17:265–279.
- Collo G, Cavalleri L, Spano PF (2014) Structural plasticity in mesencephalic dopaminergic neurons produced by drugs of abuse: critical role of BDNF and dopamine. *Front Pharmacol* 5:259.
- Colwill RM, Creton R (2011) Locomotor behaviors in zebrafish (*Danio rerio*) larvae. *Behav Processes* 86:222–229.
- Crépel V, Aronov D, Jorquera I, Represa A, Ben-Ari Y, Cossart R (2007) A parturition-associated nonsynaptic coherent activity pattern in the developing hippocampus. *Neuron* 54:105–120.
- Demarque M, Spitzer NC (2010) Activity-dependent expression of *Lmx1b* regulates specification of serotonergic neurons modulating swimming behavior. *Neuron* 67:321–334.
- Demarque M, Represa A, Becq H, Khalilov I, Ben-Ari Y, Aniksztejn L (2002) Paracrine intercellular communication by a Ca²⁺- and SNARE-independent release of GABA and glutamate prior to synapse formation. *Neuron* 36:1051–1061.
- Dulcis D, Spitzer NC (2008) Illumination controls differentiation of dopamine neurons regulating behaviour. *Nature* 456:195–201.
- Dulcis D, Jamshidi P, Leutgeb S, Spitzer NC (2013) Neurotransmitter switching in the adult brain regulates behavior. *Science* 340:449–453.
- Dulcis D, Lippi G, Stark CJ, Do LH, Berg DK, Spitzer NC (2017) Neurotransmitter switching regulated by miRNAs controls changes in social preference. *Neuron* 95:1319–1333.e5.
- Filippi A, Jainok C, Driever W (2012) Analysis of transcriptional codes for zebrafish dopaminergic neurons reveals essential functions of *Arx* and *Isl1* in prethalamic dopaminergic neuron development. *Dev Biol* 369:133–149.
- Fleming A, Diekmann H, Goldsmith P (2013) Functional characterisation of the maturation of the blood-brain barrier in larval zebrafish. *PLoS One* 8:e77548.
- Gawel K, Banono NS, Michalak A, Esguerra CV (2019) A critical review of zebrafish schizophrenia models: time for validation? *Neurosci Biobehav Rev* 107:6–22.
- Gomez TM, Spitzer NC (1999) In vivo regulation of axon extension and pathfinding by growth-cone calcium transients. *Nature* 397:350–355.
- Gomez TM, Robles E, Poo M, Spitzer NC (2001) Filopodial calcium transients promote substrate-dependent growth cone turning. *Science* 291:1983–1987.
- Goode C, Voeun M, Ncube D, Eisen J, Washbourne P, Tallafuss A (2021) Late onset of Synaptotagmin 2a expression at synapses relevant to social behavior. *J Comp Neurol* 529:2176–2188.
- Gu X, Olson EC, Spitzer NC (1994) Spontaneous neuronal calcium spikes and waves during early differentiation. *J Neurosci* 14:6325–6335.
- Guemez-Gamboa A, Xu L, Meng D, Spitzer NCC (2014) Non-cell-autonomous mechanism of activity-dependent neurotransmitter switching. *Neuron* 82:1004–1016.
- Inoue D, Wittbrodt J (2011) One for all—a highly efficient and versatile method for fluorescent immunostaining in fish embryos. *PLoS One* 6:e19713.
- Kaluff AV, et al. (2013) Towards a comprehensive catalog of zebrafish behavior 1.0 and beyond. *Zebrafish* 10:70–86.
- Klein MO, Battagello DS, Cardoso AR, Hauser DN, Bittencourt JC, Correa RG (2019) Dopamine: functions, signaling, and association with neurological diseases. *Cell Mol Neurobiol* 39:31–59.
- Lambert AM, Bonkowsky JL, Masino MA (2012) The conserved dopaminergic diencephalospinal tract mediates vertebrate locomotor development in zebrafish larvae. *J Neurosci* 32:13488–13500.
- Lange M, Norton W, Coolen M, Chaminade M, Merker S, Proft F, Schmitt A, Vernier P, Lesch K-P, Bally-Cuif L (2012) The ADHD-linked gene *Lphn3.1* controls locomotor activity and impulsivity in zebrafish. *Mol Psychiatry* 17:855.
- Li H, Pratelli M, Godavarthi S, Zambetti S, Spitzer NC (2020) Decoding neurotransmitter switching: the road forward. *J Neurosci* 40:4078–4089.
- Ma PM (1994a) Catecholaminergic systems in the zebrafish. I. Number, morphology, and histochemical characteristics of neurons in the locus coeruleus. *J Comp Neurol* 344:242–255.
- Ma PM (1994b) Catecholaminergic systems in the zebrafish. II. Projection pathways and pattern of termination of the locus coeruleus. *J Comp Neurol* 344:256–269.
- Ma PM (1997) Catecholaminergic systems in the zebrafish. III. Organization and projection pattern of medullary dopaminergic and noradrenergic neurons. *J Comp Neurol* 381:411–427.
- Ma PM (2003) Catecholaminergic systems in the zebrafish. IV. Organization and projection pattern of dopaminergic neurons in the diencephalon. *J Comp Neurol* 460:13–37.
- Macedo-Lima M, Remage-Healey L (2021) Dopamine modulation of motor and sensory cortical plasticity among vertebrates. *Integr Comp Biol* 61:316–336.
- Marek KW, Kurtz LM, Spitzer NC (2010) *CJun* integrates calcium activity and *tlx3* expression to regulate neurotransmitter specification. *Nat Neurosci* 13:944–950.
- McPherson AD, Barrios JP, Luks-Morgan SJ, Manfredi JP, Bonkowsky JL, Douglass AD, Dorsky RI (2016) Motor behavior mediated by continuously generated dopaminergic neurons in the zebrafish hypothalamus recovers after cell ablation. *Curr Biol* 26:263–269.
- Murray RM, Bhavsar V, Tripoli G, Howes O (2017) 30 years on: how the neurodevelopmental hypothesis of schizophrenia morphed into the developmental risk factor model of psychosis. *Schizophr Bull* 43:1190–1196.
- Owens DF, Kriegstein AR (1998) Patterns of intracellular calcium fluctuation in precursor cells of the neocortical ventricular zone. *J Neurosci* 18:5374–5388.
- Owens DF, Kriegstein AR (2002) Is there more to GABA than synaptic inhibition? *Nat Rev Neurosci* 3:715–727.
- Panula P, Chen YC, Priyadarshini M, Kudo H, Semenova S, Sundvik M, Sallinen V (2010) The comparative neuroanatomy and neurochemistry of zebrafish CNS systems of relevance to human neuropsychiatric diseases. *Neurobiol Dis* 40:46–57.
- Papalopolu N, Kintner C (1996) A posteriorising factor, retinoic acid, reveals that anteroposterior patterning controls the timing of neuronal differentiation in *Xenopus* neuroectoderm. *Development* 122:3409–3418.
- Plazas PV, Nicol N, Spitzer NC (2013) Activity-dependent competition regulates motor neuron axon pathfinding via PlexinA3. *Proc Natl Acad Sci USA* 110:1524–1529.
- Puttonen HAJ, Semenova S, Sundvik M, Panula P (2017) Storage of neural histamine and histaminergic neurotransmission is VMAT2 dependent in the zebrafish. *Sci Rep* 7:3060.
- Ribera AB, Spitzer NC (1998) Development of electrical excitability: mechanisms and roles. *J Neurobiol* 37:1–2.
- Scain AL, Le Corronc H, Allain AE, Muller E, Rigo JM, Meyrand P, Branchereau P, Legendre P (2010) Glycine release from radial cells modulates the spontaneous activity and its propagation during early spinal cord development. *J Neurosci* 30:390–403.
- Schweitzer J, Driever W (2009) Development of the dopamine systems in zebrafish. *Adv Exp Med Biol* 651:1–14.
- Schweitzer J, Löhr H, Filippi A, Driever W (2012) Dopaminergic and noradrenergic circuit development in zebrafish. *Dev Neurobiol* 72:256–268.

- Spitzer NC (2012) Activity-dependent neurotransmitter respecification. *Nat Rev Neurosci* 13:94–106.
- Spitzer NC, Kingston PA, Manning TJ, Conklin MW (2002) Outside and in: development of neuronal excitability. *Curr Opin Neurobiol* 12:315–323.
- Stricker D (2008) BrightStat.com: free statistics online. *Comput Methods Programs Biomed* 92:135–143.
- Tay TL, Ronneberger O, Ryu S, Nitschke R, Driever W (2011) Comprehensive catecholaminergic projectome analysis reveals single-neuron integration of zebrafish ascending and descending dopaminergic systems. *Nat Commun* 2:171.
- Thirumalai V, Cline HT (2008) Endogenous dopamine suppresses initiation of swimming in prefeeding zebrafish larvae. *J Neurophysiol* 100:1635–1648.
- Velázquez-Ulloa NA, Spitzer NC, Dulcis D (2011) Contexts for dopamine specification by calcium spike activity in the CNS. *J Neurosci* 31:78–88.
- Warp E, Agarwal G, Wyart C, Friedmann D, Oldfield CS, Conner A, Del Bene F, Arrenberg AB, Baier H, Isacoff EY, Bene F, Arrenberg AB, Baier H, Isacoff EY (2012) Emergence of patterned activity in the developing zebrafish spinal cord. *Curr Biol* 22:93–102.
- Westerfield M (2000) *The zebrafish book. A guide for the laboratory use of zebrafish (Danio rerio)*. Eugene: University of Oregon Press.
- Xavier AL, Fontaine R, Bloch S, Affaticati P, Jenett A, Demarque M, Vernier P, Yamamoto K (2017) Comparative analysis of monoaminergic cerebrospinal fluid-contacting cells in osteichthyes (bony vertebrates). *J Comp Neurol* 525:2265–2283.
- Yamamoto K, Ruuskanen JO, Wullimann MF, Vernier P (2010) Two tyrosine hydroxylase genes in vertebrates New dopaminergic territories revealed in the zebrafish brain. *Mol Cell Neurosci* 43:394–402.
- Yamamoto K, Ruuskanen JO, Wullimann MF, Vernier P (2011) Differential expression of dopaminergic cell markers in the adult zebrafish forebrain. *J Comp Neurol* 519:576–598.